Section A -Research paper

Speckle tracking Echocardiography of left ventricular function

Samaa Nabil Hassan, Salwa Mohamed ELsayed Ghoniem , Ghada Ibrahim Mohamed , Mohamed Nabil Hassan , Radwa Abdullah Elbelbesy

Cardiology Department, Faculty of Medicine, Zagazig University

Corresponding Author: Mohamed Nabil Hassan
E-Mail: gerrard.vandam@icloud.com

Article History: **Received:** 26.06.2023 **Revised:**04.07.2023 **Accepted:** 22.07.2023

DOI: 10.53555/ecb/2023.12.1061

Assessment of left ventricular systolic function is a primary component of every echocardiographic examination. The degree of systolic dysfunction is a powerful predictor of clinical outcome (**1)**

1) Left ventricular ejection fraction (EF)

Definition: The left ventricular ejection fraction (EF) is expressed as the ratio of the left ventricular stroke volume (SV) to the left ventricular end-diastolic volume (LVEDV). SV is obtained by subtracting the left ventricular end-systolic volume (LVESV) from LVEDV. Therefore, EF is calculated by the following formula**(2)**:

EF = LVEDV-LVESV /LVEDV × 100

M-mode and 2D echocardiograms are used to measure the left ventricular volume .To obtain the left ventricular volume using M-mode echocardiograms, the maximum minor axis of the left ventricle end-diastole (LVDd) and end-systole (LVDs) is measured on the parasternal long-axis or short-axis view, on the assumption that the left ventricle is a spheroid. Left ventricular volumes are usually calculated by the following formula of Teichholz (**3).**

$$v = \frac{7.0}{2.4 + D} \times D^3$$

(D= linear LV diameter)

It is acknowledged that this formula can be applied to the left ventricle that has enlarged and become almost spherical, and correlates well with the volume obtained by left ventriculography. It cannot be applied to patients whose left ventricular shapes deviate from a spheroid, and to those with regional left ventricular wall motion abnormalities during cardiac contraction (asynergy) ***(4).***

To obtain the left ventricular volumes on 2D echocardiograms:

1) The single **plane area-length** method, which calculates the volume based on the area of a single cross-section.
2) The **modified Simpson method** (disc method) are available

The biplane method of discs (modified Simpson's rule) is recommended by the ASE and the European Association of Echocardiography. This method does not assume a predetermined geometry of the LV, but instead defines the LV geometry following manual tracing of the acquired LV cavity borders. The LV volume is then

quantified by assuming the LV cavity is a stack of elliptical discs whose volumes are quantified and summated ***(5).***

Two orthogonal views—apical four-chamber and apical two-chamber—and manual tracing of endocardial borders manually traced at end systole and end-diastole are needed. Automated software divides the LV into a stack of discs oriented perpendicular to the long axis of the ventricle, and summates their individual volumes. From the end-diastolic frame, the end-diastolic volume is calculated, From the end-systolic frame, the end-systolic volume is calculated (Fig.1) ***(6).***

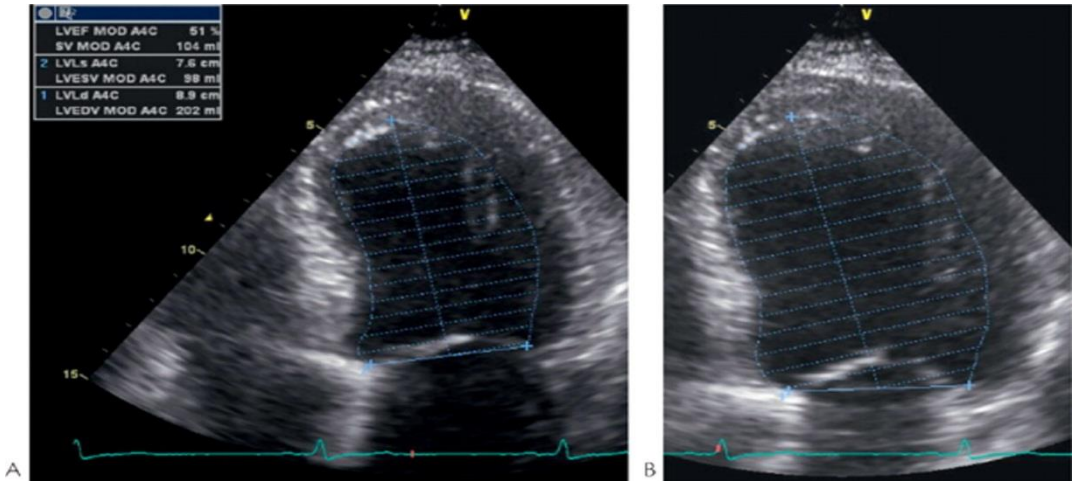

Figure. (1): Modified biplane method of discs measuring LV end diastolic and end systolic volumes ***(7)***

2) Stroke volume (SV) and stroke index(SI)

SV, the volume of blood ejected from the left ventricle during systole, is an index of the left ventricular pumping function. It is obtained by calculating the end-diastolic volume and end-systolic volume using M-mode or 2Dechocardiography as described before, and the difference between these volumes is SV ***(8)***.

Calculating stroke volume using Doppler measures:-

- In apical 5-chamber view record a PW Doppler in the outflow tract and trace the shape. Record the velocity time integral (vti).
- In a parasternal long axis view, zoom the LVOT and measure the width (edge to edge, just below aortic valve).
- Stroke volume is the area of the outflow tract ($\pi\times$ [LVOT diameter/2]^2) multiplied by the outflow tract VTI ***(9).***

When assessing SV value as an index of left ventricular function, it should be recognized that the cardiac output and SV can be maintained by dilating the left ventricle even in patients with impaired myocardial systolic function ***(10).***

3) Cardiac output (CO) and cardiac index (CI)

CO, the volume of blood ejected from the left ventricle to the aorta per minute, is an index of the left ventricular pumping function that is obtained by

multiplying the stroke volume by the heart rate per minute. The cardiac index is obtained by dividing the cardiac output by the body surface area to correct for body size (**11**).

4) Left ventricular percent fractional shortening (%FS)

Left ventricular %FS is an index of systolic function that is obtained by measuring the left ventricular end-diastolic dimension and left ventricular end-systolic dimension, dividing the difference by the left ventricular end-diastolic dimension, and shown as percentage in accordance with the following formula:

$$FS = \frac{LVDd - LVDs}{LVDd} \times 100\ \%$$

A normal value is between 30% and 50% ***(12).***

5) Myocardial Performance Index

The myocardial performance index (MPI, also known as "Tei" index) is an expression of global ventricular performance. It is a simple calculation that includes both systolic and diastolic parameters and can be applied to either the left or right ventricle. The MPI incorporates three basic time intervals that are readily derived from Doppler recordings:

- The ejection time (**ET**) .
- Isovolumic contraction time (**IVCT**).
- The isovolumic relaxation time (**IVRT**).

From these values, the MPI can be calculated from the following formula***(13)***:

MPI = (IVCT + IVRT) / ET

Systolic dysfunction is associated with a prolongation of IVCT and a shortening of the ET. Therefore, this will result in an increase in the MPI, the normal range is 0.39 ± 0.05, and values above 0.50 are considered abnormal ***(14).***

6) Left Ventricular Mass, Geometry, and Relative Wall Thickness (RWT) (15)

a) LV Mass = 1.05 (Total LV volume – LV Chamber volume)

Normally indexed to BSA :

(women = 44-88 g/m2, men = 50-102 g/m2)

b) RWT = 2 × (Inferolateral Wall Thickness)/LVInternal Diameter***(16).***

- Performed in diastole
- Normal Geometry= Normal LV mass and RWT
- Concentric Hypertrophy = ↑ LV mass and ↑ RWT
- Eccentric Hypertrophy = ↑ LV mass with Normal RWT
- Concentric Remodeling = Normal LV mass and ↑ RWT

7) Left ventricular dP/dt

dP/dt describes the rise in intraventricular pressure during early systole The change in pressure is determined by systolic contraction so the faster the rise the better the left ventricular systolic function ***(17).***

Measure the time taken for the velocity of the mitral regurgitant jet to rise from 1 to 3m/s (the measure has been standardized for this pressure rise from 4 to 36 mmHg). The machine or software will normally automatically calculate dP/dt if the 1m/s and 3m/s points are marked. dP/dt > 1200mmHg/s relates to normal function and <800mmHg/s (roughly > 40ms) is severely depressed function ***(18)***.

8) Regional wall motion assessment

Echocardiography, with its high spatial and temporal resolution, is an ideally suited non-invasive method of assessing wall motion. In suspected acute coronary syndrome (ACS) wall motion abnormality (WMA) precedes changes on the ECG and symptoms and hence is extremely useful in the early detection of ACS. Conversely in patients with suspected ACS with inconclusive ECGs, normal WM excludes ischaemia ***(19).***

Assessment of regional wall motion :

Left ventricular wall motion is assessed in the apical 4-, 2-, 3-chamber, parasternal long and short axis views. This allows complete visualisation of all the left ventricular walls, and hence all 3 vascular territories, although care must be taken to ensure clear endocardial border definition. Clear visualisation of the endocardial border is crucial for the full assessment of wall motion ***(20).***

Wall motion and wall thickening assessments are described in Table 1.

Table 1: Methods for Evaluation of Regional Wall Motion Abnormalities***(21)*** :

Visual/subjective **normal, hypokinetic, akinetic, dyskinetic**
Semiquantiative **WMS or WMSI** **1. = normal** **2. = hypokinetic, i.e. reduced endocardial excursion and wall thickening** **3. = akinetic, absent endocardial excursion and thickening** **4. = dyskinetic, systolic bulging with no thickening** **WMSI = Total score of segments/Total number of segments.** **WMS, wall motion score; WMSI, wall motion score index**

Tissue Doppler Imaging (TDI)

DI images low-velocity, high amplitude myocardial velocity signals and is obtained by pulsed Doppler or colour Doppler (CTDI) . CTDI acquires tissue velocity information from the entire sector and thus multiple sites can be interrogated simultaneously and analysed offline ***(22).***

TDI has been validated extensively in a variety of cardiac pathologies including HF, AMI, hypertension, diabetes and in stress echocardiography where TDI systolic velocities are used as an adjunct to WMSI ***(23)***.

The systolic motion of the mitral annulus toward the apex (Sm) is a sensitive marker of impaired LV systolic function, even in those with a normal LVEF. Sm velocity is a predictor of outcomes and in patients with cardiac disease , mortality was higher when Sm was < 3 cm/s. In HF patients, CTDI Sm velocity and diastolic arterial pressure were independent predictors of outcome ***(24).***

9) Speckle Tracking echocardiography :

Discussed later

Evaluation of Diastolic Function:

Echocardiography has been the mainstay for understanding the physiology of diastolic function, and identifying the pathophysiology of diastolic dysfunction Fig. 2***(25)***

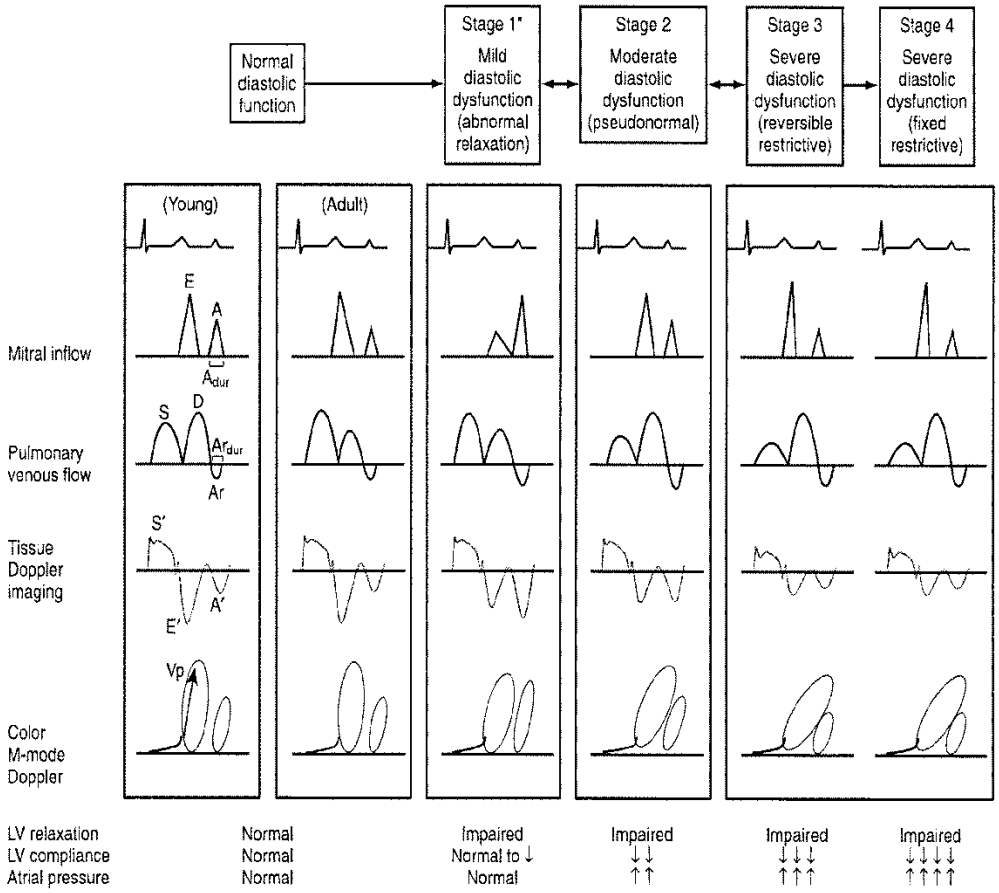

Figure (2) Stages of diastolic dysfunction Schematic representation of the typical patterns seen with mitral inflow, pulmonary venous flow, tissue Doppler echocardiography, and color M-mode propagation velocity (*Vp*) for normal (young and adult), impaired relaxation, pseudonormal , and restrictive diastolic function. The stages of diastolic dysfunction can be determined using an integrated approach with these four different modalities for assessment of diastolic flow pattern ***(26).***

Table (2) : Criteria used to define grades of diastolic dysfunction (27).

Criteria	***Normal Young***	***Normal Adult***	***Impaired Relaxation (Grade 1)***	***Pseudonormal (Grade 2)***	***Restrictive Reversible (Grade 3)***	***Restrictive Irreversible (Grade 4)***
E/A ratio	1-2	1-2	<1.0	1-1.5 (reverses with Valsalva maneuver)	>1.5	1.5-2.0
Deceleration time (ms)	<240	150-240	≥240	150-200	<150	<150
IVRT (ms)	70-90	70-90	0>90	<90	<70	<70
PV S2/D ratio	<1	≥1	≥1	<1	<1	<1
Ardur – Adur (ms)	≥30	≤0	≤0or≥30	≥30	≥30	≥30
Ar velocity (cm/s)	<35	<35	<35	≥35	≥35	≥35
Propagation velocity (cm/s)	>55	>55	>45	<45	<45	<45
Mitral E′velocity (cm/s)	>10	>8	<8	<8	<8	<8
Left atrium	Normal	Normal	Normal or mildly enlarged LA	Mild to moderate LA enlargement	Severe LA enlargement	Severe LA enlargement

Doppler techniques in assessment of diastolic filling patterns

There is a large body of scientific evidence validating the typical patterns of diastolic filling in normal subjects, and those with diastolic dysfunction. These filling patterns are generally not characteristic of a particular disease process, but represent the end product of a complex set of pathophysiologic events. Furthermore, these patterns can also be affected by operator-related issues (e.g., precise placement of the sample volume) and physiologic factors (e.g., heart rate and volume status) and are not a reflection of true diastolic function ***(28).***

(1) Transmitral Flow Assessment :

The most traditional technique of assessment of LV filling patterns involves using pulsed-wave Doppler mitral flow velocity recordings. The following are the variables derived from mitral inflow interrogation:

- peak early diastolic transmitral flow velocity (E).
- peak late diastolic transmitral flow velocity (A).
- early filling deceleration time (DT).
- Awave duration (Adur) **(29).**

There are many factors that affect the transmitral velocity waveform; among them are heart rate and rhythm, aging, and preload. As the heart rate increases, time for diastasis is reduced, the A wave occurs earlier and its maximum velocity is increased. At rates of greater than 100 beats/min fusion of the E wave and A waves occurs resulting in monophasic diastolic filling. In atrial fibrillation the A wave is lost and the height of the E wave is determined by the length of the preceding cardiac cycle ***(30).***

Normal individuals demonstrate a rapidly accelerating E wave, relatively rapid deceleration, and an A wave significantly smaller than the E wave. The E/A ratio is greater than 1. With normal aging, there is slowing of LV relaxation and, hence, a gradual decrease of the peak E wave velocity, and an increase of A wave peak velocity. In most individuals, E and A waves become approximately equal in the sixth decade of life ***(31).***

The evolution of traditional diastolic parameters with progressively worsening diastolic function, occurs in the following manner: For patients with diastolic dysfunction, three abnormal filling patterns are initially recognized ***(32).***

In stage 1 diastolic dysfunction (abnormal relaxation) :

There is Prolongation to IVRT (greater than 90 ms) as LV pressure falls slowly. The early LA/LV pressure gradient is therefore relatively low and this is reflected in a diminished E wave maximal velocity. As early filling is decreased, LA volume is larger at the time of atrial contraction and this results in a higher A wave. There is reversal of the normal E/A ratio (less than 1) and deceleration time is prolonged (greater than 240 ms). These findings are associated with a low pulmonary capillary wedge pressure (15mmHg) ***(30).***

Stage 2 diastolic dysfunction, or pseudonormal pattern :

Results from a combination of impaired relaxation and elevated filling pressures is associated with a normal appearance of the transmitral inflow with an E/A ratio between 1 and 1.5, a DT between 160 and 240 ms, and an IVRT between 60 and 100 ms ***(33).***

Stage 3 diastolic dysfunction or restrictive filling:

With disease progression, occurs when there is a high LA pressure and a non distensible Ventricle ,there is a very high E wave, a low A wave, and a significantly decreased DT. The E/A ratio is usually greater than 2 with a DT less than 160 ms, and IVRT less than 70 ms. These findings reflect a high LA pressure at MV opening, and rapid filling of the LV that terminates rapidly. The A wave is low velocity due to either atrial dysfunction or a high LVEDP***(26).***

Stage 4:

Further observations have subcategorized this last pattern to either reversible or fixed restrictive pattern (stage 4) depending on the response to the Valsalva maneuver or other preload reducing maneuvers ***(34).***

The major challenge in the interpretation of Doppler mitral inflow patterns is in distinguishing the normal from the pseudonormal pattern. To accurately assess and stratify the degree of diastolic abnormality, further measurements are generally necessary. There are several traditional methods that are useful in distinguishing normal from pseudonormal patterns, including the Valsalva maneuver, pulmonary venous (PV) flow measurements, and the tissue Doppler annular velocities (E′) Fig. (3) ***(28).***

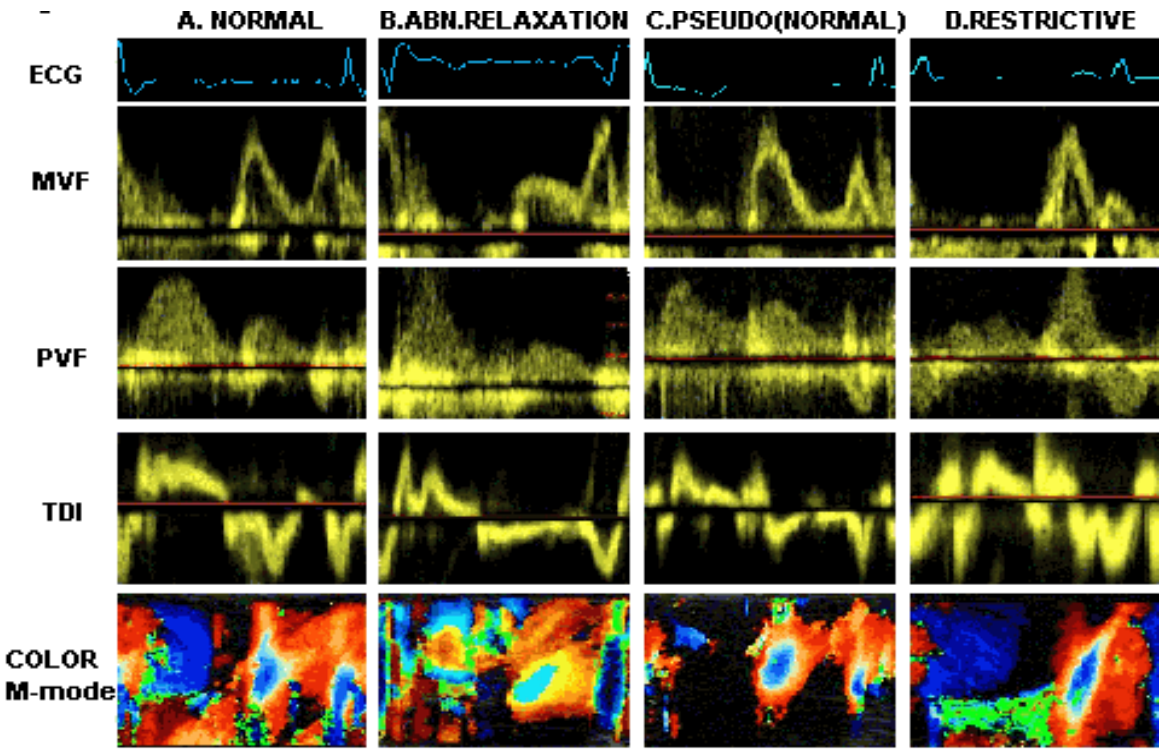

Figure (3) different patterns of diastolic dysfunction *(35).*

(2) Pulmonary Venous Flow

PV flow velocity variables provide an integrated approach with mitral inflow in the evaluation of diastolic dysfunction. The four useful variables from the PV flow interrogation are peak systolic PV flow velocity (S), peak diastolic PV flow velocity (D), peak PV atrial reversal flow velocity (PVa), and PVa duration (adur)***(30)***.

The S wave may be biphasic, the early phase (Se) attributed to LA relaxation and the later (Sl) associated with apical displacement of the MV annulus. The D wave is associated with MV opening and LV filling prior to atrial contraction. Atrial contraction forces blood into the LV but also retrograde into the pulmonary veins So the flow from the PV to the LA occurs in three phases:

- systolic phase (peak early and late systolic PV flow velocity) .
- early diastolic phase (peak diastolic PV flow velocity).
- retrograde flow during the late diastole with atrial contraction.

The S wave is higher in normal subjects than the D wave and when it is biphasic Sl will be higher than Se The ratio of S velocity to D velocity is approximately 1.3–1.5 in normals with the S flow velocity integral occupying 60–68% of the total flow velocity integral. As with the transmitral E and A waves, pulmonary vein S and D waves may fuse at high heart rates, and as with the transmitral flow, age related changes have been described. The D wave decreases and the Ar and S wave increase with advancing age ***(36).***

As LA pressure rises its compliance is diminished. The magnitude of the S wave is primarily related to LA compliance and therefore the pulmonary vein systolic fraction (the proportion of the total pulmonary venous flow velocity integral contributed by the S wave) is inversely related to mean LA pressure. With a normal LA pressure, the majority of the flow into LA occurs in systole. However, when the mean LA pressure increases, the majority of the antegrade flow occurs in diastole with a concomitant reduction in systolic flow. A decreased systolic fraction of less than 40% is associated with an elevated mean LA pressure greater than 15 mmHg ***(8).***

(3)Tissue-Doppler Imaging for Evaluation of Diastolic Function

Doppler tissue imaging (DTI), also known as tissue Doppler imaging (TDI), enables the measurement of the high amplitude, low velocity signals of myocardial motion, rather than blood flow velocities as with standard Doppler interrogation **(29)**.

The main advantage of DTI information is that it is less load-dependant than standard Doppler. The assessment of early myocardial relaxation velocities provides an additional window on LV diastolic function in a manner complementary to evaluation of mitral inflow and PV flow patterns ***(37).***

Thus, a cardiac cycle is represented by three waveforms

1) Sa, systolic myocardial velocity above the baseline.
2) Ea, early diastolic myocardial relaxation velocity below the baseline.
3) Aa, myocardial velocity associated with atrial contraction, below the baseline. The subscripts "a" for annulus or "m" for myo- cardial (Ea or Em) or the superscript "prime" (E′) are used to differentiate tissue Doppler velocities from the corresponding standard Doppler blood flow velocities***(38).***

Normal values for é at the medial mitral annulus are from 10 cm/s to 15 cm/s and those at the lateral annulus are from 15 cm/s to 20 cm/s. The E- peak velocity is higher than the A velocity in normals and like the transmitral E wave, E- decreases with age. E- velocity is reduced in diastolic dysfunction but does not change with variations in preload ***(39).***

A normal ratio of E/é is <8. The ratio does not change with impaired relaxation as both E and é are reduced. As diastolic function deteriorates , the LA pressure rises causing an increase in E but no change in é. The E/ é ratio continues to increase with the appearance of a restrictive pattern of transmitral flow caused by further increases in LA pressure. The E/ é ratio has also been used to predict LV filling pressure. An E/ é ratio < 8 accurately predicts a normal mean LV end diastolic pressure (LVEDP) and an E/é ratio of >15 accurately predicts a mean LVEDP of >15mmHg. However, intermediate values of E/ é are associated with a wide variation in mean LVEDP***(40).***

Reduction in lateral Ea velocity less than 8–10 cm/sec is an indication of impaired LV relaxation. In contrast to standard mitral flow inflow patterns, Ea velocities tend to remain consistently reduced through all phases of diastolic dysfunction. In addition to assessing diastolic function, Ea velocities can be used to estimate LV filling pressures, to discriminate between constrictive pericarditis and restrictive cardiomyopathy, and to differentiate athlete's heart from hypertrophic cardiomyopathy (HCM) **(41).**

Estimation of LV filling pressures:

Several investigators have performed simultaneous cardiac catheterization and echocardiographic studies to estimate LV filling pressures using the ratio of the mitral inflow E-wave and the tissue Doppler Ea-wave. Different regression formulas have been proposed to calculate either LV end diastolic pressure (LVEDP) or pulmonary capillary wedge pressure. Perhaps more practical than specific regression formulae is the correlation with the ratio of E/Ea alone. E/Ea more than 10–15 correlates with an elevated LVEDP (>12 mmHg).E/Ea less than 8 correlates with a normal LVEDP Fig. (4 & 5) ***(42)***.

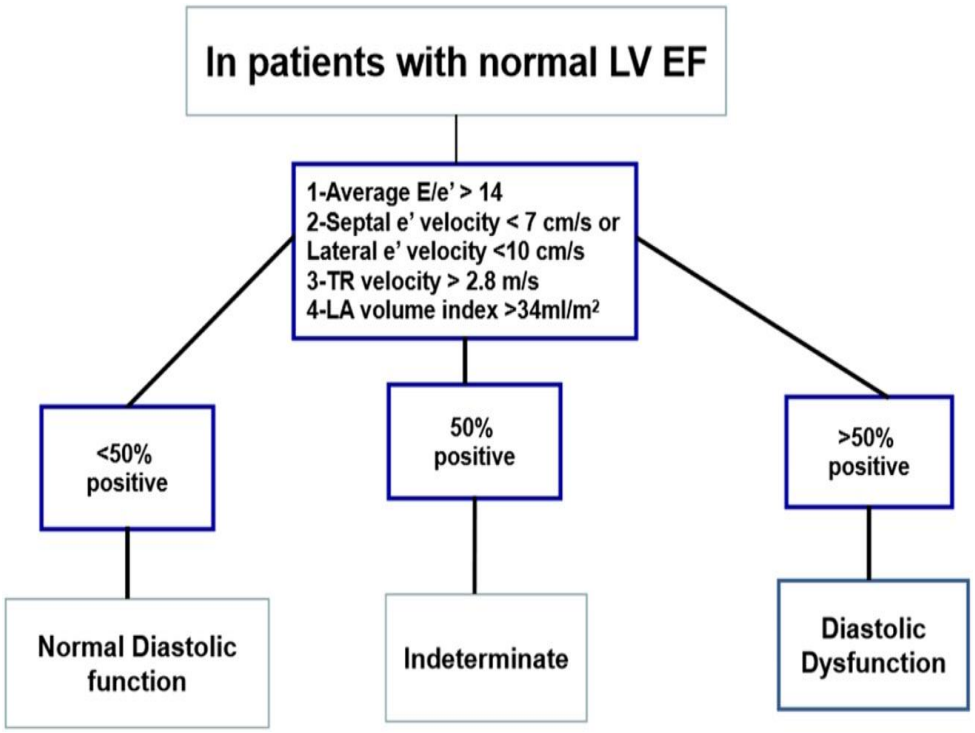

Figure (4) Diagnostic algorithm for the estimation of LV filling pressures in patients with normal ejection fraction ***(26)***

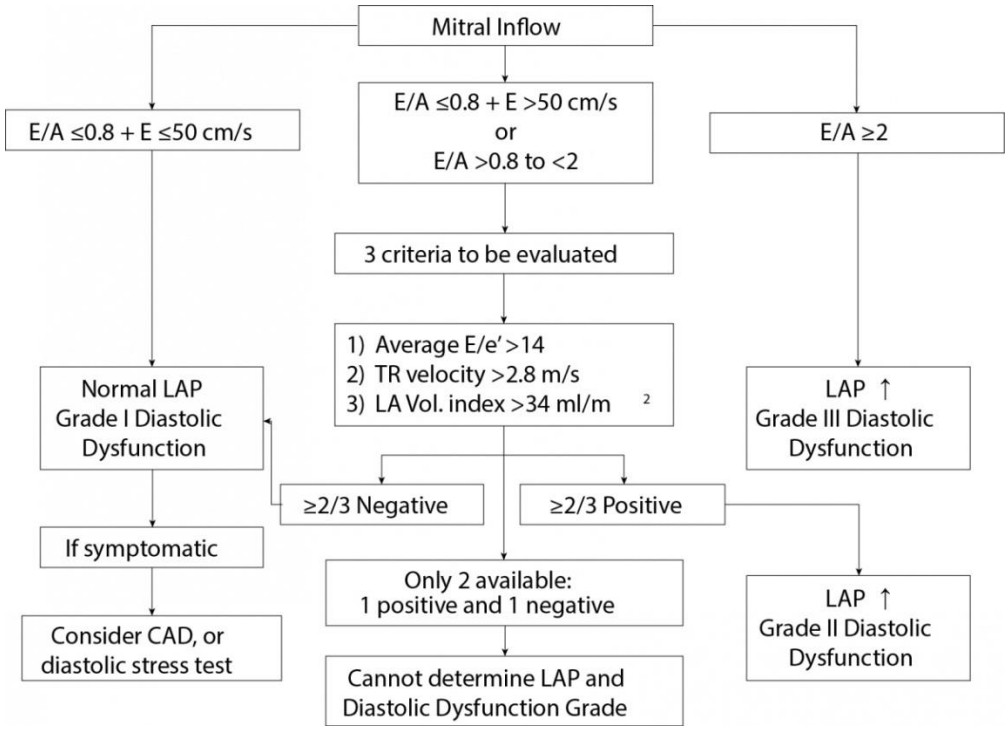

Figure (5) Diagnostic algorithm for the estimation of pressures in patients with depressed ejection fraction **(26).**

(4) Color M-Mode

Color M-mode Doppler imaging from the apical four-chamber window is an alternative method to relate mitral inflow to LV relaxation, again in a less load dependent manner than standard transmitral Doppler The velocity of propagation of flow (Vp) from the LV base toward the apex is measured in early diastole. The slope of this flow signal is thought to represent the LV intraventricular gradient, influenced by active recoil (suction forces) and relaxation. This is accomplished by measuring the slope of the leading edge of flow (the transition from black to color) or an isovelocity line (e.g., the first aliasing velocity line). Normal Vp exceeds 55 cm per second. Vp less than 45 cm per second is thought to indicate impaired relaxation***(43).***

Speckle tracking echocardiography

Speckle-tracking echocardiography has emerged as a quantitative technique for evaluating myocardial function through analyzing the motion of speckles identified on 2-dimensional echocardiograms ***(44).***

It provides non-Doppler, angle-independent, and objective analysis of myocardial deformation and left ventricular systolic and diastolic functions***(8).***

By tracking the displacement of the speckles during the different phases of cardiac cycle, the strain and strain rate can be rapidly measured offline after adequate acquisition of images. Data regarding the accuracy, feasibility and clinical applications of speckle-tracking are rapidly accumulating ***(44).***

Speckle-tracking echocardiography provides semi-automated information of myocardial deformation in the 3 spatial directions: longitudinal, circumferential and radial. Also provides data of left ventricle (LV) rotation ***(45).***

Before the introduction of this sophisticated echocardiographic technique, only magnetic resonance imaging (MRI) had been used for analysis of the several deformation components that characterize myocardial dynamics ***(44).***

Although speckle tracking was introduced for the analysis of LV function, its use has been extended to be applicable to other cardiac chambers, as right ventricle, left and right atrium ***(26).***

Terminology and Definition

- **Strain(ε)**

A measure that evaluates the degree of deformation of analyzed segment in relation to its initial dimensions and expressed as a percentage. The strain equation (ε) is as follows:

$$\varepsilon = (L-L_0)/L_0 = \Delta L/L_0$$

L; length of the object after deformation,

L_0; the basal length of the object.

Depending on the direction, lengthening or thickening deformation gives a positive value, whereas a shortening or thinning deformation gives a negative one ***(46).***

❖ **Strain Rate** (ε′)

The strain rate (ε′) represents the myocardial deformation in relation to time. It is expressed as seconds. Strain rate is less dependent on LV load variations than strain. However, because the strain rate signal is noisier and less reproducible, most of the clinical studies still use strain measurements $\varepsilon` = \Delta\varepsilon/\Delta t = (\Delta L/L_0)/\Delta t = (\Delta L/(\Delta t)/L_0 = \Delta V/L_0$, Where ΔV; is the velocity gradient in the segment studied***(44).***

❖ **Longitudinal Strain**

It represents myocardial deformation directed from the base to the apex. Through longitudinal strain analysis in 4-chamber, 2-chamber, and 3- chamber views, regional and global strain values can be measured. Global longitudinal strain (GLS) has been validated as a quantitative index for global LV function (Fig.6). The same measurement can be applied to the analysis of myocardial deformation of the left atrium and right ventricle ***(15).***

❖ **Circumferential Strain**

Represents LV myocardial fiber shortening along the circular perimeter on a short-axis view. Circumferential strain is represented by negative curves. Also, it is possible to obtain a global circumferential strain value (GCS) (Fig.7) ***(47).***

❖ **Radial Strain**

Represents myocardial deformation toward the center of the LV cavity, indicating the LV thickening and thinning motion during the cardiac cycle. Radial strain values are obtained by speckle-tracking analysis of basal, mid and apical LV short-axis views, radial strain is represented by positive curves (Fig.8) ***(48).***

❖ **Left Ventricular Torsion/twist**

A component of the normal LV systolic contraction arising from the reciprocal rotation of the LV apex and base during systole. Left ventricular torsion is calculated as the net difference rotation between the apical and basal segments, Fig 9 ***(26).***

❖ **Untwisting**

Untwisting velocity is thought to be a critical manifestation of active relaxation, which makes it a relevant investigation for diastole and, mainly, isovolumic relaxation because it is less load dependent compared to other diastolic parameters ***(49).***

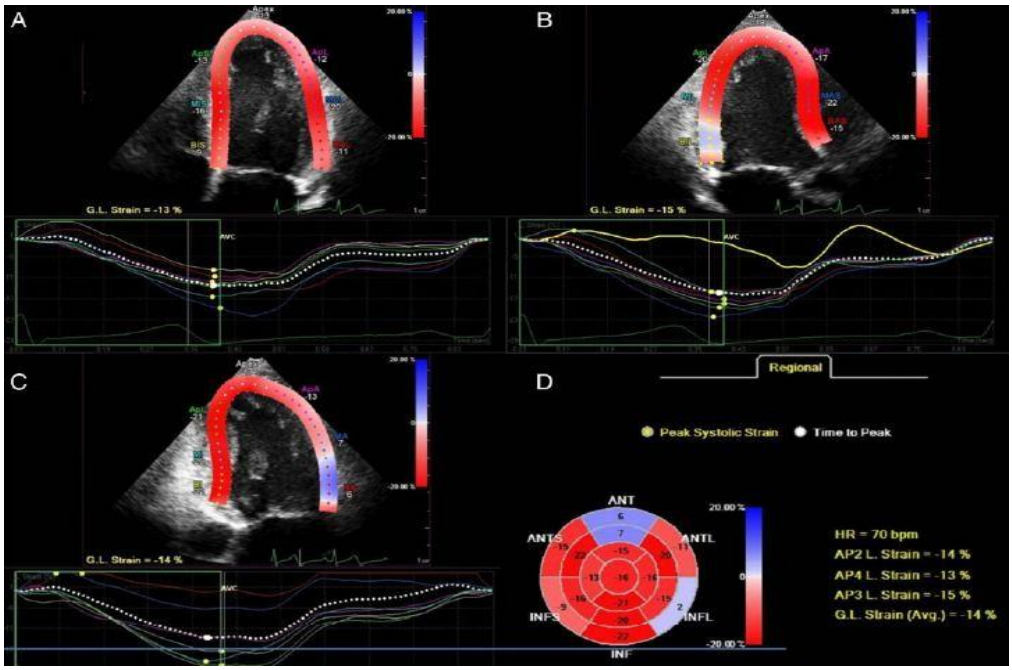

Figure (6): Longitudinal strain acquired from AP4C, AP2C and AP3C AP4C: apical four chamber, AP2C: apical two chamber, AP3C: apical three chamber and GLS: global longitudinal strain ***(50).***

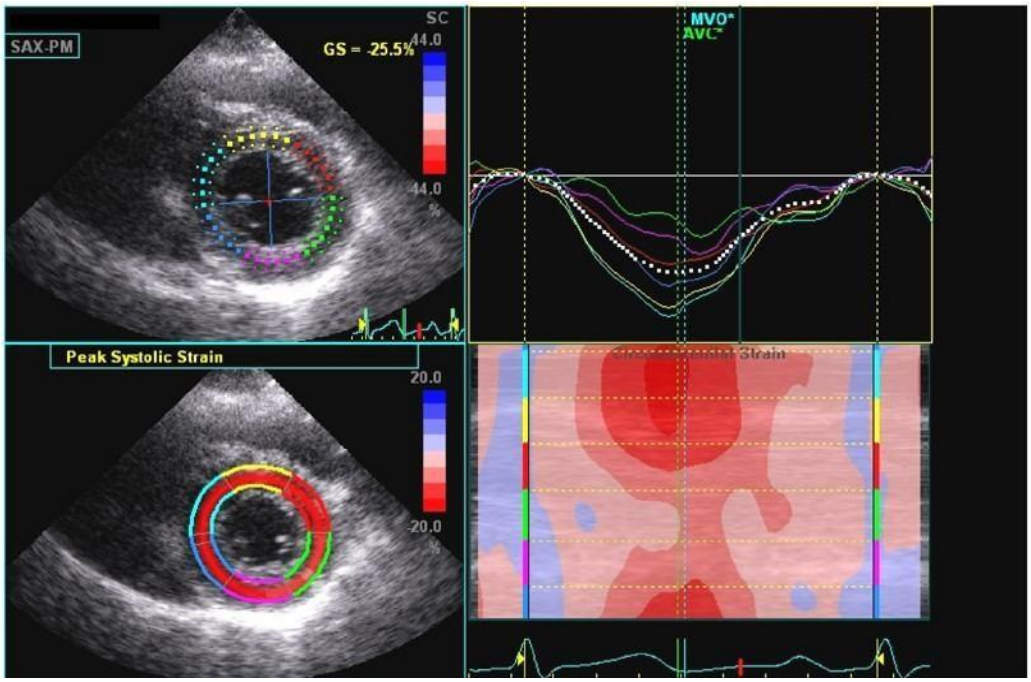

Figure (7): Circumferential strain acquired from SAX, PM level SAX PM: short axis, papillary muscle level ***(51).***

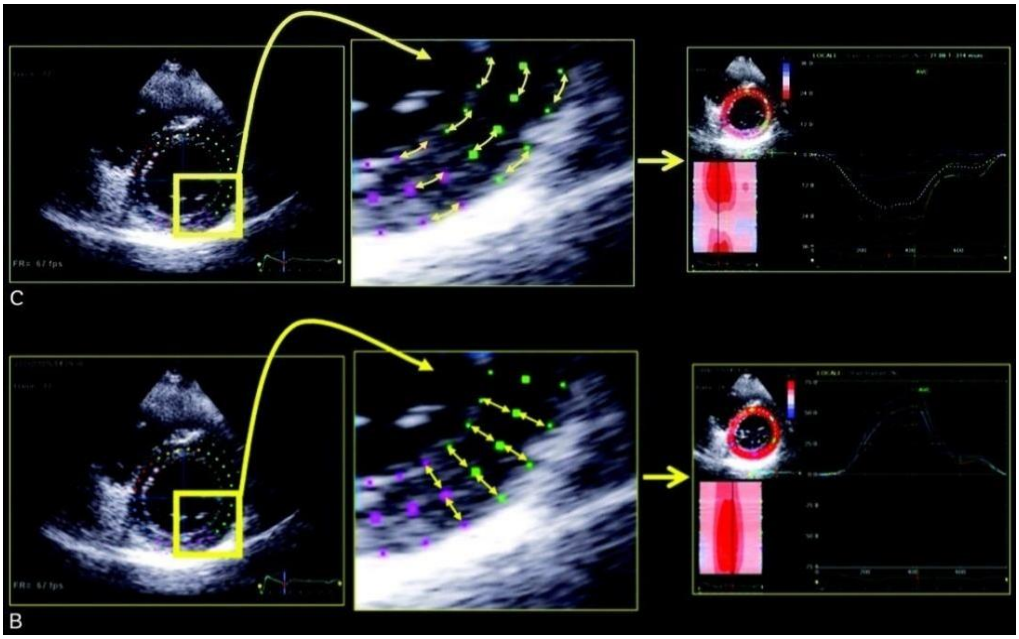

Figure (8) Speckle-tracking echocardiographic analysis of myocardial deformation showing measurements of radial strain and circumferential strain ***(52).***

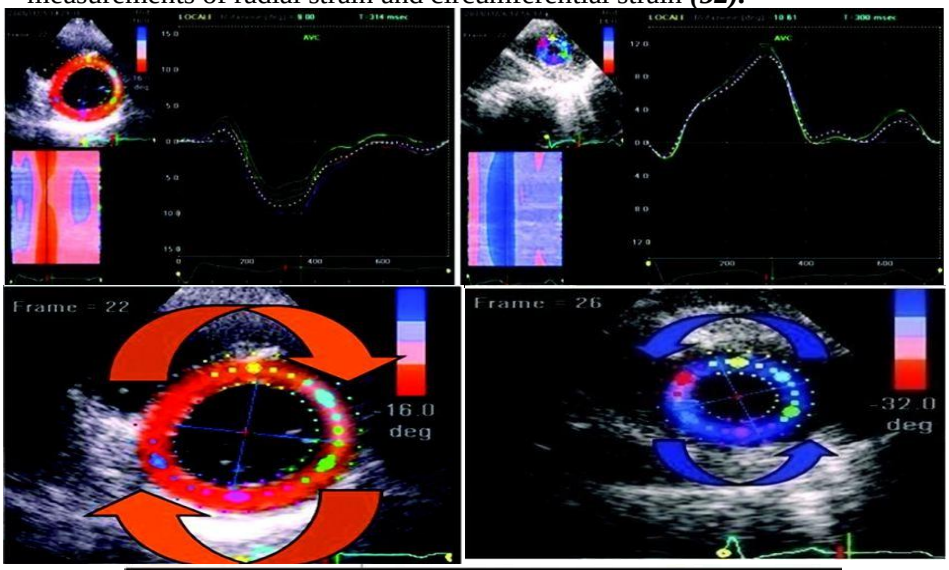

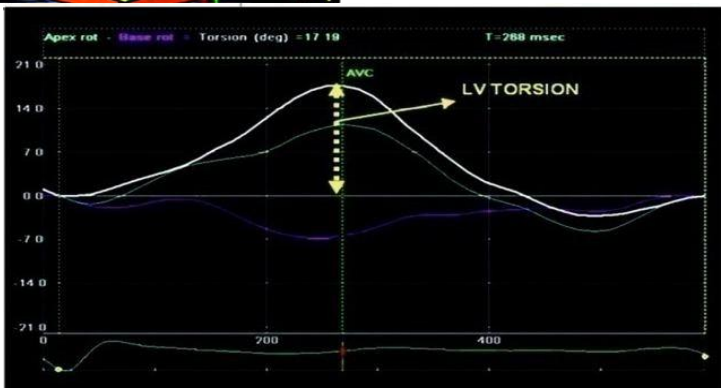

Figure (9) Graphic depiction of left ventricular rotational dynamics showing rotation of the cardiac base (left) and apex (right). In the bottom panel, a diagram of left ventricular (LV) torsion measurement is represented as the net difference between mean apical and basal rotation; AVC indicates aortic valve closure ***(44).***

Clinical

Applications:

In general, speckle-tracking echocardiography allows further data of myocardial systolic and diastolic dynamics beyond traditional echocardiographic techniques ***(53).***

A. Hypertension:

Arterial hypertension is an ideal model for assessing the changes in different varieties of deformation occurring hand in hand with the development of LV concentric geometry.

This is a crucial issue because experiences using standard echocardiography have shown that impairment of mid wall fractional shortening of the circumferential fibers precedes the reduction of the LVEF. Speckle-tracking echocardiography has helped in the understanding that the interaction of the different deformations is much more complex. In particular, it seems that longitudinal and radial strain are impaired when circumferential strain and LV torsion is still normal, acting as a compensatory mechanisms to preserve a normal ejection fraction (EF) ***(54).***

B. Diabetes mellitus:

In asymptomatic diabetic patients with normal LVEF, Speckle- tracking echocardiography can detect subclinical LV systolic dysfunction before the overt appearance of diabetic cardiomyopathy ***(55).***

C. Coronary Artery Disease:

Recent studies reported that a lower longitudinal strain value in asymptomatic patients without wall motion abnormalities is a strong predictor of stable coronary artery disease. In acute myocardial infarction recent studies have showed that longitudinal strain is related to the levels of cardiac troponin T and to the infarct size***(56).***

In addition, it has been shown that a cut off value of −4.5% for regional longitudinal strain discriminates between segments with a viable myocardium and those with transmural scar tissue on contrast-enhanced MRI, with sensitivity of 81.2% and specificity of 81.6%***(57).***

D.Heart Failure:

Recent studies on heart failure with preserved ejection fraction have reported that LV longitudinal strain progressively deteriorates from NYHA class I to class IV, also LV radial and circumferential systolic impairment occurring in NYHA classes III and IV. Studies also showed that systolic twisting, torsion, and diastolic untwisting are significantly increased in patients with mild diastolic dysfunction ***(58).***

In heart failure with reduced ejection fraction a recent study has found global circumferential strain to be a powerful predictor of cardiac events ***(59).***

E. Identification of Subclinical Dysfunction During Chemotherapy

Cardiac toxicity remains an important side effect of chemotherapeutic agents, early detection of cardiac injury is important because it may facilitate early therapeutic measures. Speckle-tracking echocardiography has been shown to reliably detect preclinical abnormalities in regional and global myocardial function ***(60).***

F. Mechanical Dyssynchrony:

CRT is an effective treatment option for patients with NYHA class II, III and ambulatory class IV heart failure patient with LVEF of ≤ 35% and QRS prolongation who remain symptomatic despite optimal medical therapy ***(61).***

However, about 30% of patients fail to show a satisfactory response to cardiac resynchronization therapy, and several studies have been made to recognize non responders before implantation. A variety of echocardiographic parameters to predict the response to CRT have been tested ***(62).***

In a multicenter trial, none of the conventional and tissue Doppler-based echocardiographic indices of dyssynchrony was shown to be a reliable predictor of the response to CRT ***(63).***

Prospective randomized trials for predicting the responders to CRT therapy by speckle tracking echocardiography are still lacking ***(64).***

G. Heart Transplantation:

Recent study reported impairment in LV twisting, torsion, and untwisting rates in heart transplant recipients in comparison to age-matched controls and to patients underwent other types of cardiac surgeries Fig (10)

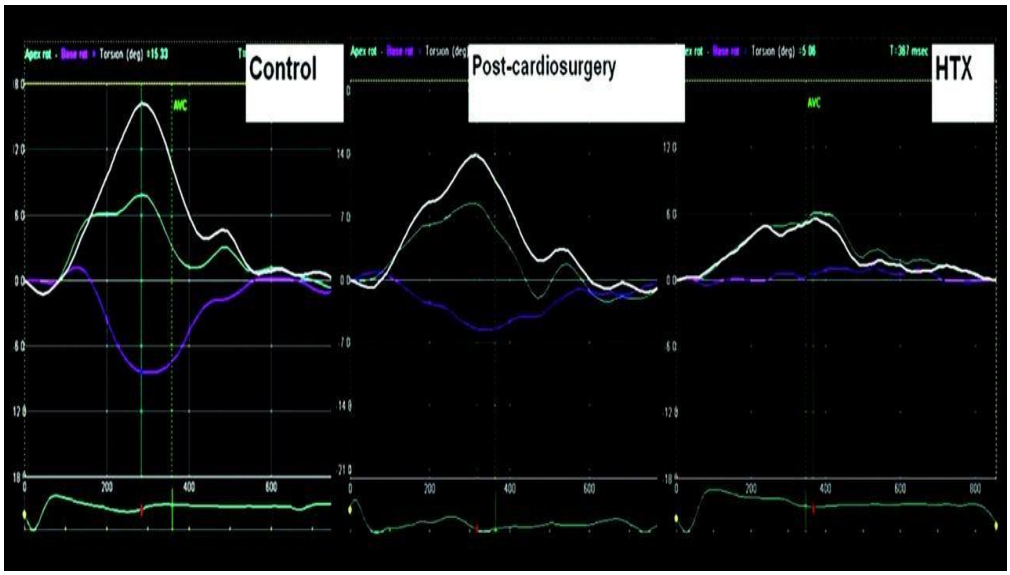

Figure (10): Comparative representation of left ventricular twisting measurements in an age-matched healthy individual (left), a patient after non-transplant cardiac surgery (middle), and in a heart transplant (HTX) recipient (right). The ventricular twisting function appears strongly reduced after heart transplantation ***(65).***

H. Left Atrial Function:

Preliminary data on of the peak atrial longitudinal strain suggested that arterial hypertension and diabetes have a major impact on LA function, even in absence of LA enlargement that further impairs LA performance in an additive manner Fig.(11) ***(66).***

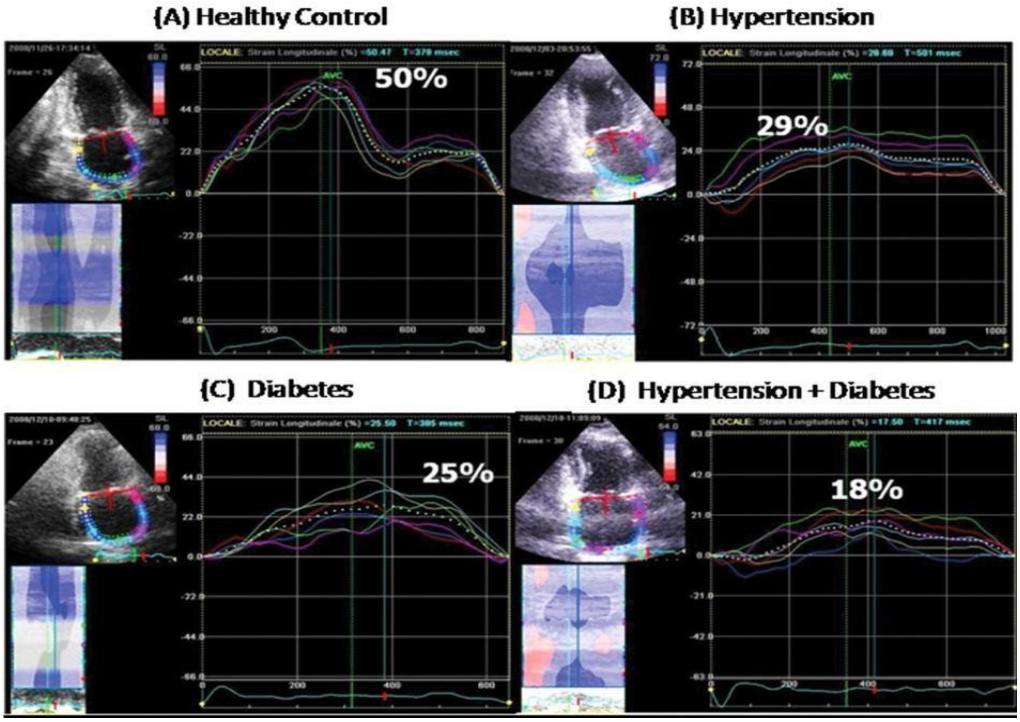

Figure (11): Left atrial function analysis by speckle-tracking echocardiography showing sample peak atrial longitudinal strain measurements in a healthy individual (**A**), a hypertensive patient (**B**), a diabetic patient (**C**), and a hypertensive and diabetic patient (**D**) with a preserved ejection fraction and no enlargement of the left atrium. Both hypertension and diabetes have a major impact on left atrial myocardial deformation. Coexistence of both conditions further impairs left atrial performance in an additive manner ***(44)*.**

Limitations of 2D speckle tracking:

All speckle-tracking–derived measurements require more capability in image acquisition, obtaining correct endocardial border delineation, obtaining suitable echocardiographic views, interobserver and intra observer variability. Furthermore, it is not suitable in patients with non-sinus rhythms. And also the results depend critically on the machine with which the analyses are performed***(67)*.**

References:

1. **von Bibra & Sutton.** Diastolic dysfunction in diabetes and the metabolic syndrome: promising potential for diagnosis and prognosis, Diabetologia, 2010, 53(6), 1033-45.
2. **Cheang, Barber, Hauser, et al.** A comprehensive characterization of myocardial and vascular phenotype in pediatric chronic kidney disease using cardiovascular magnetic resonance imaging. Journal of Cardiovascular Magnetic Resonance, 2018, 20(1), 24.
3. **Inui, Izumi, Kubota, et al.** Extracellular volume fraction assessed using cardiovascular magnetic resonance can predict improvement in left ventricular ejection fraction in patients with dilated cardiomyopathy. Heart and vessels, 2018, 33(10), 1195-203.
4. **Yoneyama, Nakajima, Okuda, et al.** Reducing the small-heart effect in pediatric gated myocardial perfusion

single-photon emission computed tomography. Journal of Nuclear Cardiology, 2017, 24(4), 1378-88.

5. **Chiu.** Cardiac Risk Assessment Using 2D and 3D Transthoracic Echocardiography in Patients Undergoing Haemodialysis. The University of Manchester (United Kingdom) 2016.
6. **Oh & Kane.** The Echo Manual: Ebook without Multimedia. Lippincott Williams & Wilkins, 2018.
7. **Foley, Mankad, Anavekar, et al.** Measuring left ventricular ejection fraction–techniques and potential pitfalls. Eur Cardiol, 2012, 8(2), 108-14.
8. **Cameli, Mondillo, Righini, et al.** Echocardiographic assessment of left ventricular systolic function: from ejection fraction to torsion. Heart failure reviews, 2016, 21(1), 77-94
9. **Teeter, Conti, Wasicek, et al.** Feasibility of basic transesophageal echocardiography in hemorrhagic shock: potential applications during resuscitative endovascular balloon occlusion of the aorta (REBOA). Cardiovascular ultrasound, 2018, 16(1), 12.
10. **Noordegraaf, Westerhof, Westerhof, et al.** The relationship between the right ventricle and its load in pulmonary hypertension. Journal of the American College of Cardiology, 2017, 69(2), 236-43 .
11. **Appleton, C. P., Firstenberg, M. S., Garcia, M. J., & Thomas, J. D. (2000).** The echo-Doppler evaluation of left ventricular diastolic function: a current perspective. Cardiology clinics, 18(3), 513-546.
12. **Genoni, G., Menegon, V., Secco, G. G., Sonzini, M., Martelli, M., Castagno, M., ... & Prodam, F. (2017).** Insulin resistance, serum uric acid and metabolic syndrome are linked to cardiovascular dysfunction in pediatric obesity. International journal of cardiology, 249, 366-371.
13. **Alhakak, A. S., Olsen, F. J., Skaarup, K. G., Lassen, M. C. H., Johansen, N. D., Jørgensen, P. G., ... & Biering-Sørensen, T. (2023).** Age- and sex-based normal reference ranges of the cardiac time intervals: the Copenhagen City Heart Study. Clinical Research in Cardiology, 1-13.
14. **Hashemi, N. (2018).** *Novel Insights into Echocardiographic Assessment of Cardiac Function Following Heart Surgery* (Doctoral dissertation, Karolinska Institutet (Sweden)).
15. **Lang, Badano, Afilalo, et al**. Recommendations for cardiac chamber quantification by echocardiography in adults: an update from the American Society of Echocardiography and the European Association of Cardiovascular Imaging . European Heart Journal-Cardiovascular Imaging, 2015, 16(3), 233-71
16. **Avenatti, E., Rebellato, A., Iannaccone, A., Battocchio, M., Dassie, F., Veglio, F., ... & Fallo, F. (2017).** Left ventricular geometry and 24-h blood pressure profile in Cushing's syndrome. *Endocrine*, *55*, 547-554.

17. **Chengode.** Left ventricular global systolic function assessment by echocardiography. Annals of cardiac anaesthesia, 2016, 19.Suppl 1, S26.
18. **Pierard, Luc, Marie Moonen, et al.** Valvular regurgitation. The ESC Textbook of Cardiovascular Imaging, 2010, 149-76.
19. **Nihoyannopoulos, Petros & Jean Louis Vanoverschelde.** Myocardial ischaemia and viability: the pivotal role of echocardiography. European heart journal, 2011, 32.7, 810-9.
20. **Jeetley, Khattar & Senior.** Coronary Artery Disease: Assessing Regional Wall Motion. In Echocardiography, 2018, (pp. 451-66): Springer, Cham.
21. **Youssef, Saad, Ammar, et al.** Assessment of left ventricular regional wall motion abnormalities using regional time-volume curves obtained by real time three-dimensional echocardiography. The Egyptian Heart Journal, 2018, 70(3), 189-94.
22. **Garcia, Rodriguez, Ares, et al**. Myocardial wall velocity assessment by pulsed Doppler tissue imaging: characteristic findings in normal subjects, American heart journal, 1996, 132(3), 648-56.
23. **Ponikowski, Voors, Anker, et al.** ESC Guidelines for the diagnosis and treatment of acute and chronic heart failure: The Task Force for the diagnosis and treatment of acute and chronic heart failure of the European Society of Cardiology (ESC). Developed with the special contribution of the Heart Failure Association (HFA) of the ESC. European journal of heart failure, 2016, 18(8), 891-975.
24. **Sulemane, Bratsas, Grapsa, et al.** Subclinical markers of cardiovascular disease predict adverse outcomes in chronic kidney disease patients with normal left ventricular ejection fraction. The international journal of cardiovascular imaging, 2017, 33(5), 687-98.
25. **McLean, Zhabyeyev, Wang, et al.** PI3Kα Pathway Inhibition With Doxorubicin Treatment Results in Distinct Biventricular Atrophy and Remodeling With Right Ventricular Dysfunction. Journal of the American Heart Association, 2019, 8(9), e010961 .
26. **Nagueh, Appleton, Gillebert, et al.** Recommendations for the evaluation of left ventricular diastolic function by echocardiography. European Journal of Echocardiography, 2009, 10(2), 165-93.
27. **Clancy, D. J., Scully, T., Slama, M., Huang, S., McLean, A. S., & Orde, S. R. (2017).** Application of updated guidelines on diastolic dysfunction in patients with severe sepsis and septic shock. *Annals of intensive care*, *7*(1), 1-10.
28. **Mitter, Shah, Thomas, et al.** A test in context: E/A and E/e′ to assess diastolic dysfunction and LV filling pressure. Journal of the American College of Cardiology, 2017, 69(11), 1451-64
29. **Tadi, Lehtonen, Saraste, et al.** Gyrocardiography: A new non-invasive monitoring method for the assessment of cardiac mechanics and

the estimation of hemodynamic variables. Scientific reports , 2017, 7(1), 6823.

30. **Silbiger.** Pathophysiology and echocardiographic diagnosis of left ventricular diastolic dysfunction . Journal of the American Society of Echocardiography, 2019, 32(2), 216-32.
31. **Shinmura, Tamaki, Sano, et al.** Impact of long-term caloric restriction on cardiac senescence: caloric restriction ameliorates cardiac diastolic dysfunction associated with aging. Journal of molecular and cellular cardiology, 2011, 50(1), 117-27.
32. **Bianco, Farjo, Ghaffar, et al.** Myocardial Mechanics in Patients With Normal LVEF and Diastolic Dysfunction. JACC: Cardiovascular Imaging, 2019.
33. **Habib, Bucciarelli-Ducci, Caforio, et al.** Multimodality imaging in restrictive cardiomyopathies: an European association of cardiovascular imaging expert consensus document in collaboration with the "Working group on myocardial and pericardial diseases" of the European Society of Cardiology endorsed by the Indian Academy of Echocardiography. Journal of The Indian Academy of Echocardiography & Cardiovascular Imaging, 2018, 2(1), 19.
34. **Pablo-Kaski J & Elliott P**. Hypertrophic, Dilated, and Restrictive Cardiomyopathies. Principles and Practice of Clinical Cardiovascular Genetics, 2010; 189.
35. **Schnelle, M., Catibog, N., Zhang, M., Nabeebaccus, A. A., Anderson, G., Richards, D. A., ... & Shah, A. M. (2018).** Echocardiographic evaluation of diastolic function in mouse models of heart disease. *Journal of molecular and cellular cardiology*, *114*, 20-28.
36. **Schober, Karsten & Valerie Chetboul.** Echocardiographic evaluation of left ventricular diastolic function in cats: hemodynamic determinants and pattern recognition. Journal of Veterinary Cardiology 17, 2015, S102-33.
37. **Pasipoularides.** Evaluation of right and left ventricular diastolic filling. Journal of cardiovascular translational research, 2013, 6(4), 623-39.
38. **Ghista, Dhanjoo, Liang Zhong, et al.** Cardiac Function Assessment in Filling and Systolic Phases: Passive and Active Elastances of the Left Ventricle. Cardiology Science and Technology, 2016, CRC Press, 77-100.
39. **Sun, Yang, Guo, et al.** Left atrial regional phasic strain, strain rate and velocity by speckle-tracking echocardiography: normal values and effects of aging in a large group of normal subjects. International journal of cardiology,2013, 168(4), 3473-9.
40. **Bergerot, Davidsen, Amaz, et al.** Diastolic function deterioration in type 2 diabetes mellitus: predictive factors over a 3-year follow-up. European Heart Journal-Cardiovascular Imaging, 2017, 19(1), 67-73.

41. **Shah & Shah.** Multidimensional assessment of diastolic dysfunction using echocardiography and magnetic resonance imaging in acute coronary syndrome 2015.
42. **Knežević, Musić, Bulatović, et al.** Systolic and diastolic function in hypertension. Age, 2015, 59, 10.087.
43. **Mayank Kansal, Bansal, Jagat Narula, et al.** Imaging in advanced heart failure. Oxford Textbook of Advanced Heart Failure and Cardiac Transplantation, 2016, 102.
44. **Mondillo, Galderisi , Mele, et al.** Speckle-tracking echocardiography : a new technique for assessing myocardial function. Journal of Ultrasound in Medicine, 2011; 30(1), 71-83.
45. **Blessberger & Binder.** Two dimensional speckle tracking echocardiography: basic principles. Heart, 2010, 96(9), 716-22
46. **Lillie.** Development, Validation, and Clinical Application of a Numerical Model for Pulse Wave Velocity Propagation in a Cardiovascular System with Application to Noninvasive Blood Pressure Measurements 2017.
47. **Esposito, Sorrentino, Galderisi, et al.** The use of transthoracic echocardiography for the assessment of left ventricular systolic and diastolic function in patients with suspected or ascertained chronic heart failure. Expert review of cardiovascular therapy, 2016, 14(1), 37-50.
48. **Nagata , Takeuchi, Izumo, et al.** Prognostic value of LV deformation parameters using 2D and 3D speckle-tracking echocardiography in asymptomatic patients with severe aortic stenosis and preserved LV ejection fraction. JACC: Cardiovascular Imaging, 2015, 8(3), 235-45.
49. **Notomi Y, Popovic Z B, Yamada H, et al**. Ventricular untwisting: a temporal link between left ventricular relaxation and suction, 2008.
50. **Levy, Debry, Labescat, et al.** Echocardiographic prediction of postoperative atrial fibrillation after aortic valve replacement for aortic stenosis: a two-dimensional speckle tracking left ventricular longitudinal strain multicentre pilot study. Archives of cardiovascular diseases, 2012, 105(10), 499-506.
51. **Marcus, Mavinkurve-Groothuis, Barends, et al.** Reference values for myocardial two-dimensional strain echocardiography in a healthy pediatric and young adult cohort. Journal of the American Society of Echocardiography, 2011, 24(6), 625-36.
52. **Hare, Brown, Leano, et al.** Use of myocardial deformation imaging to detect preclinical myocardial dysfunction before conventional measures in patients undergoing breast cancer treatment with trastuzumab. American heart journal, 2009, 158(2), 294-301.
53. **Biswas, Sudhakar, Buckberg, et al.** Two-and three-dimensional speckle tracking echocardiography: clinical applications and future directions.

Echocardiography, 2013, 30(1), 88-105 .

54. **Galderisi, Henein , Roelandt, et al.** Recommendations of the European Association of Echocardiography How to use echo-Doppler in clinical trials: different modalities for different purposes. European Journal of Echocardiography, 2011, 12(5), 339-53.
55. **Geyer, Caracciolo, Wilansky, et al.** Assessment of myocardial mechanics using speckle tracking echocardiography: fundamentals and clinical applications. Journal of the American Society of Echocardiography, 2010, 23(4), 351-69.
56. **Kalam, Otahal & Marwick.** Prognostic implications of global LV dysfunction: a systematic review and meta-analysis of global longitudinal strain and ejection fraction. Heart, 2014, 100(21), 1673-80.
57. **Gorcsan & Tanaka.** Echocardiographic assessment of myocardial strain. Journal of the American College of Cardiology, 2011, 58(14), 1401-13 .
58. **Imbalzano, Zito, Mandraffino, et al.** Left ventricular function in hypertension: new insight by speckle tracking echocardiography. Echocardiography, 2011, 28(6), 649-57.
59. **Ersbøll, Andersen, Velazquez, et al.** Prediction of all-cause mortality and heart failure admissions from global left ventricular longitudinal strain in patients with acute myocardial infarction and preserved left ventricular ejection fraction. Journal of the American College of Cardiology, 2013, 61(23), 2365-73.
60. **De Geus-Oei, Bellersen, Gotthardt , et al.** Scintigraphic techniques for early detection of cancer treatment–induced cardiotoxicity, Journal of Nuclear Medicine, 2011, 52(4), 560-71 .
61. **Dickstein, Filippatos, Ponikowski, et al .** ESC Guidelines for the diagnosis and treatment of acute and chronic heart failure 2008: The Task Force for the Diagnosis and Treatment of Acute and Chronic Heart Failure 2008 of the European Society of Cardiology. Developed in collaboration with the Heart Failure Association of the ESC (HFA) and endorsed by the European Society of Intensive Care Medicine (ESICM) . European journal of heart failure, 2008, 10(10), 933-89.
62. **Foley, Sanderson, Frenneaux, et al.** Cardiac resynchronisation therapy in patients with heart failure and a normal QRS duration: the RESPOND study. Heart, 2011, 97(13), 1041-7.
63. **Leenders, Cramer, Doevendans, et al** . Echocardiographic prediction of outcome after cardiac resynchronization therapy: conventional methods and recent developments. Heart Fail Rev. 2011, 16(3), 235-50.
64. **Saba, Marek , Schwartzman, et al.** Echocardiography-guided left ventricular lead placement for cardiac resynchronization therapy: results of the Speckle Tracking Assisted Resynchronization Therapy for

Electrode Region trial, Circulation: Heart Failure, 2013, 6(3), 427-34.

65. **Veress & Gabriella.** New Echocardiographic Techniques in Rare Cardiological Disorders, Doctoral dissertation, 2012.
66. **Donal, Goette, Marwan, et al.** EACVI/EHRA Expert Consensus Document on the role of multi-modality imaging for the evaluation of patients with atrial fibrillation European Heart Journal–Cardiovascular Imaging, 2016, 17(4), 355-83.
67. **Kempny, Orwat, Schuler, et al.** Quantification of biventricular myocardial function using cardiac magnetic resonance feature tracking, endocardial border delineation and echocardiographic speckle tracking in patients with repaired tetralogy of Fallot and healthy controls. Journal of Cardiovascular Magnetic Resonance, 2012, 14(1), 32.